Numerical Simulation of the Flow Past a Pair of Magnetic Obstacles

J. Román, A. Beltrán and S. Cuevas

Abstract We present a quasi-two-dimensional numerical simulation of the flow of a thin layer of electrolyte past a pair of localized Lorentz forces, named *magnetic obstacles*, placed side by side. Opposing Lorentz forces are produced by the interaction of the magnetic field created by a pair of small permanent magnets and a D.C. current applied tranversally to the main flow. By varying the separation between the magnets and the intensity of the applied current, different flow regimes are analyzed. The attention is focused on the interference of the wakes created by the magnetic obstacles.

1 Introduction

The flow past solid obstacles is certainly one of the most widely studied problems in fluid dynamics and constitutes in itself a classic subject of research (Zdravkovich 1997). Its importance stems from countless applications where determining the behavior of flows past bluff bodies is of practical interest. From the point of view of dynamical system, the understanding of the spatio-temporal behavior of the wakes formed in flows past solid obstacles presents interesting challenges. When more than one obstacle is present, investigating the interference of wakes becomes a relevant issue (Gal et al. 1996). In fact, the behavior of coupled wakes created by a pair of cylinders placed side by side in a uniform flow has been studied experimentally and theoretically by several authors and different flow regimes have been identified according to the separation between the cylinders (Zdravkovich 1985; Le Gal et al. 1990; Peschard and Gal 1996; Sumner et al. 1999). But, wakes are not only

J. Román · S. Cuevas (✉)
Instituto de Energías Renovables, Universidad Nacional Autónoma de México,
A.P. 34, Temixco, 62580 Morelos, México
e-mail: scg@ier.unam.mx

A. Beltrán
Instituto de Investigaciones en Materiales, Unidad Morelia,
Universidad Nacional Autónoma de México, Antigua Carretera a Pátzcuaro No. 8701,
Col. Ex Hacienda de San José de la Huerta, 58190 Morelia, MICH, Mexico

J. Klapp et al. (eds.), *Selected Topics of Computational and Experimental Fluid Mechanics*, Environmental Science and Engineering,
DOI 10.1007/978-3-319-11487-3_31

produced by solid obstacles. It has been shown that localized magnetic forces in flows of electrically conducting fluids act as obstacles for the flow. When the conducting fluid is a liquid metal, the relative motion of the fluid and a localized magnetic field induces electric currents that interact with the same field to produce a Lorentz force braking the liquid (Cuevas et al. 2006; Votyakov et al. 2007). In the case of an electrolyte, due to the low conductivity of the fluid, induced currents are negligible but an opposing Lorentz force can still be created if an electric current is externally applied (Honji 1991; Honji and Haraguchi 1995; Afanasyev and Korabel 2006). In both cases, experimental and theoretical studies have shown the appearance of different flow regimes such as steady vortices, vortex shedding, and even turbulent wakes (Honji and Haraguchi 1995; Afanasyev and Korabel 2006; Votyakov et al. 2008; Kenjeres et al. 2011). In fact, the term *magnetic obstacle* was coined (Cuevas et al. 2006) to emphasize that localized Lorentz forces produce flow behaviors that in some aspects resemble flows past solid obstacles, although very important differences exist.

So far, investigations of flows past magnetic obstacles have mainly addressed the problem of a single obstacle in liquid metal flows (see, for instance, Votyakov et al. 2008; Kenjeres et al. 2011; Tympel et al. 2013). Recently, the flow in an array of three magnetic obstacles has been simulated numerically (Kenjeres 2012), a situation that may have relevance for heat transfer applications (Zhang and Huang 2013). Flows of electrolytes past magnetic obstacles have been less explored. Honji (1991) and Honji and Haraguchi (1995) performed experiments in a shallow layer of salt water contained in a long tank, where a D.C. current was applied transversally to the tank's long axis, while a permanent magnet located externally was dragged at a constant velocity along the center line of the water tank. Similarly, more extensive experiments were performed by Afanasyev and Korabel (2006). These authors considered flows produced by a single magnet as well as by two magnets with opposite orientations, aligned with the direction of motion and separated by a short distance. However, to the best of our knowledge, the electrolytic flow created by a pair of magnetic obstacles side by side has not been previously considered. This problem is interesting, since the analogous flow with solid obstacles has been investigated extensively so that flow regimes are well characterized (Zdravkovich 1985; Peschard and Gal 1996; Sumner et al. 1999). In the present paper, we explore numerically the flow past a pair of magnetic obstacles side by side and compare the flow regimes with those corresponding to the flow past solid cylinders.

2 Formulation of the Problem

We consider the flow of a shallow layer of an electrolyte in a rectangular container affected by localized Lorentz forces, i.e. magnetic obstacles. The forces are produced by the interaction of magnetic fields generated by two permanent magnets and a D.C. electrical current applied transversally to the main flow through electrodes located in the lateral walls and connected to a power source. Square magnets whose side length

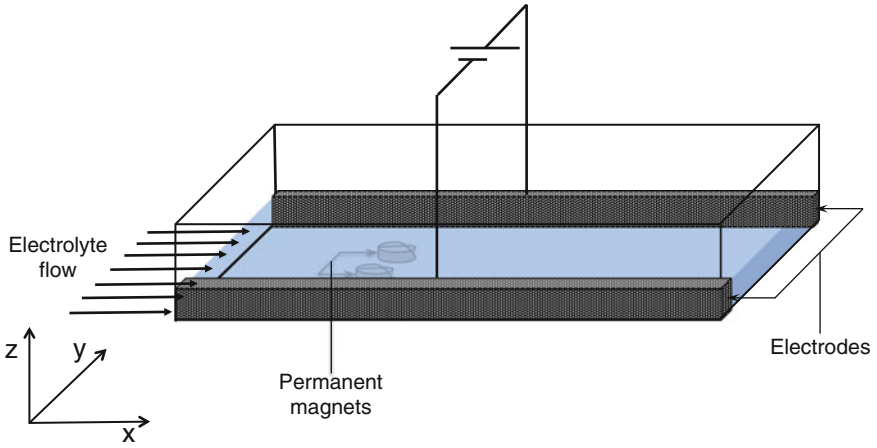

Fig. 1 Sketch of the electrolytic flow past a pair of magnetic obstacles side by side. See details in the text

L is much smaller than the distance between lateral walls, are placed beneath the bottom wall of the container with an orientation such that resulting Lorentz forces oppose the oncoming flow and generate vorticity. Figure 1 shows a sketch of the problem under consideration. Since the thickness of the fluid layer is assumed to be small compared with horizontal dimensions, we use a quasi-two-dimensional (Q2D) numerical model that only considers the component of the applied magnetic field normal to the plane of motion. This component can be expressed as

$$B_z^0(x, y, z) = B(x, y)g(z), \tag{1}$$

where $B(x, y)$ reproduces the variation of the magnetic field in the x–y plane and is modeled by a dipolar field distribution created by a square magnetized surface uniformly polarized in the normal direction, for which an explicit analytical expression is available (McCaig 1977; Cuevas et al. 2006). In fact, the shape of the magnets is irrelevant provided the plane of flow is separated from the surface of the magnet, so that border effects are smoothed out (Figueroa et al. 2009). In turn, $g(z) = \exp(-\gamma z)$ models the decay of the magnetic field in the normal direction z (normalized by the layer thickness h), where $\gamma = 0.51$ is an empirical constant obtained from fitting the decay of the magnetic field in the vertical direction (Beltrán 2010) with experimental data from a permanent magnet (Honji 1991). In addition, the Q2D model assumes that the momentum transfer through the thin electrolytic layer is mainly diffusive so that the velocity field can be expressed as

$$\mathbf{u}(x, y, z, t) = [\overline{u}(x, y, t)f(x, y, z), \overline{v}(x, y, t)f(x, y, z), 0], \tag{2}$$

where $\overline{u}$ and $\overline{v}$ are the mean velocity components in the x–y plane, while $f(x, y, z)$ reproduces the velocity profile in the layer thickness (Beltrán 2010). Since the electrical conductivity of the electrolyte is low compared with that of liquid metals, and the magnetic field intensity of permanent magnets is weak, induced currents in the fluid are negligible. Therefore, it becomes unnecessary to solve the induction equation to determine the induced magnetic field. Only the applied current is relevant for calculating the Lorentz forces (Figueroa et al. 2009).

Substituting Eqs. (1) and (2) in the three-dimensional equations of motion and averaging along the height of the fluid layer, we obtain the Q2D equations. A detailed description of the averaging procedure can be found in (Beltrán 2010; Figueroa et al. 2009). In dimensionless terms, the equations of motion in the Q2D approximation take the form

$$\frac{\partial u}{\partial x} + \frac{\partial v}{\partial y} = 0, \tag{3}$$

$$\frac{\partial u}{\partial t} + \left(u\frac{\partial u}{\partial x} + v\frac{\partial u}{\partial y} \right) = -\frac{\partial P}{\partial x} + \frac{1}{Re}\nabla_{\perp}^2 u + \frac{u}{\tau} - Q B_z^0, \tag{4}$$

$$\frac{\partial v}{\partial t} + \left(u\frac{\partial v}{\partial x} + v\frac{\partial v}{\partial y} \right) = -\frac{\partial P}{\partial y} + \frac{1}{Re}\nabla_{\perp}^2 v + \frac{v}{\tau}, \tag{5}$$

where the overline in the velocity components was dropped and subindex $\perp$ denotes the projection of the ∇ operator on the x–y plane. The velocity components, u and v, the pressure, P, the applied current density, j, and the applied magnetic field, B_z^0, are normalized by U, ρU^2, J_0 and B_{max}, respectively. Here, U is the uniform entrance velocity, ρ is the mass density, B_{max} is the maximum intensity of the magnetic field, and J_0 is the magnitude of the applied current density. Dimensionless coordinates x and y are normalized by L, while time, t, is normalized by L/U. Dimensionless parameters Re and Q stand for the Reynolds number $Re = UL/\nu$, where ν is the kinematic viscosity, and the Lorentz force parameter $Q = J_0 B_{max} L/\rho U^2$ which is the ratio of a magnetic pressure drop caused by the applied Lorentz force and the free-stream dynamic pressure. Essentially, Q characterizes the strength of the Lorentz forces. The third term on the right-hand-side of Eqs. (4) and (5) represents the Rayleigh friction between the fluid and the bottom wall. It involves a characteristic dimensionless timescale, τ, for the decay of vorticity due to dissipation in the viscous layers and is given by (Beltrán 2010)

$$\tau^{-1} = \frac{\gamma(1 - \mathrm{e}^{-\gamma})}{\frac{1}{\gamma}(1 - \mathrm{e}^{-\gamma}) + \frac{\gamma}{2}\mathrm{e}^{-\gamma} - 1}. \tag{6}$$

The considered boundary conditions are the following. At the entrance, a uniform flow is imposed in the x-direction, therefore

$$u = 1, \qquad v = 0, \qquad \text{at } x = 0, \quad 0 \le y \le H. \tag{7}$$

At the outlet, Neumann boundary conditions are used, that is,

$$\frac{\partial u}{\partial x} = \frac{\partial v}{\partial x} = 0, \qquad \text{at } x = X_L, \qquad 0 \le y \le H. \tag{8}$$

At the side walls, we use no-slip conditions:

$$u = 0, \qquad v = 0, \qquad \text{at } \; y = 0, H, \qquad 0 \le x \le X_L. \tag{9}$$

Here, H is the separation between lateral boundaries which determines the solid blockage of the confined flow, characterized by the blockage parameter $\beta = 1/H$. In turn, X_L is the total length of the channel. The magnetic obstacles are located at distances X_u from the entrance and X_d from the outlet. All the lengths are measured in dimensionless units. The centers of the magnets are separated by a dimensionless distance $D = d/L$, where d is the dimensional separation. Figure 2 shows a sketch of the flow conditions considered for the numerical solution.

A finite volume method implemented with a SIMPLEC algorithm is used to solve the governing equations (3)–(6) with boundary conditions (7)–(9). The diffusive and convective terms are discretized using a central difference scheme. Accurate temporal resolution is provided by choosing a small enough time step and employing a second order scheme for the time integration. The numerical solution was obtained in a rectangular domain with a length of $X_L = 35$ dimensionless units in the streamwise direction and $H = 7$ units in the cross-stream direction using an equidistant orthogonal grid of 212×202 nodes. It was determined that an upstream distance $X_u = 10$ and a downstream distance $X_d = 25$ guarantee results that are nearly independent of the location of the obstacles.

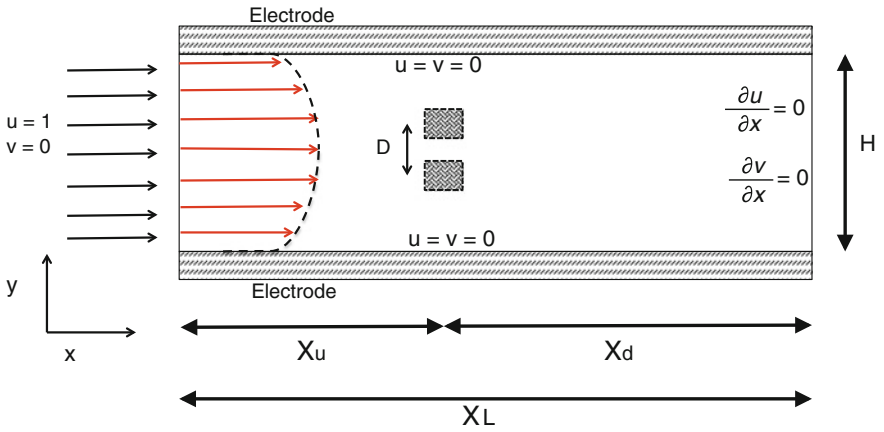

Fig. 2 Sketch of the geometry and boundary conditions considered for the analyzed flow

3 Numerical Results

In a similar way as when the obstacles are solid cylinders, flows past a pair of magnetic obstacles side by side present different regimes according to the flow conditions. While hydrodynamic regimes are governed only by the Reynolds number and the dimensionless separation distance D (provided three-dimensional effects are neglected), in the present case flow regimes are controlled by Q, in addition to Re and D. The variation of these parameters leads to steady or time-dependent regimes, as occurs in flows with a single magnetic obstacle (Honji and Haraguchi 1995; Afanasyev and Korabel 2006). We present numerical results for a pair of magnetic obstacles side by side with a fixed Reynolds number, $Re = 1{,}000$, and investigate the variation of Q and D on the flow dynamics. We consider flow conditions where vortex shedding is present and explore the effect of separation distance D on the coupling of the wakes behind the obstacles. The parameter Q is varied in the range $1.5 \leq Q \leq 10$, and for a given D, the value of Q corresponds to the minimum value where vortex shedding appears. In turn, four different values of D are explored, namely, 1, 1.5, 2, and 3, which are of interest since results for the hydrodynamic flow past a pair of solid obstacles are available in the literature for these cases (Peschard and Gal 1996; Zdravkovich 1985).

In hydrodynamic flows, it has been reported that for large distances between the cylinders, the pair of wakes presents a weak coupling where in phase and out of phase vortex shedding can appear. In turn, for shorter distances a strong coupling arises and only in phase shedding is observed which produces a unique von Kármán street (Peschard and Gal 1996; Zdravkovich 1985). At intermediate range of coupling, a bistable regime can emerge which is characterized by a biased flow that gives two possible values for the vortex shedding frequency. The biased flow is an intermittent flow between two asymmetric states. That is, through the gap the biased flow divides asymmetric states with narrow and wide wakes which can intermittently interchange between the two cylinders (Zdravkovich 1985), apparently driven by a random process (Peschard and Gal 1996). We now show that similar regimes are observed in the wakes created by a pair of magnetic obstacles side by side.

Figure 3 shows the Lagrangian tracking of flows obtained numerically for different values of D, with the corresponding minimum value of Q where vortex shedding appears. For the smallest separation distance, $D = 1$ (see Fig. 3a), the magnets are in contact and act as a larger magnetic obstacle that gives rise to a single wake similar to the von Kármán street. If the gap between the obstacles is increased to $D = 1.5$, we find a bistable regime where the flow pattern is rather complex, as is observed in Fig. 3b. A further increase to $D = 2$ (see Fig. 3c) leads to a more structured flow pattern with two interlaced wakes in phase. For the larger gap explored, namely $D = 3$, the separation between the wakes is neatly defined and the in phase behavior still persists, as observed in Fig. 3d.

To improve the understanding of the flow behavior and the coupling of the wakes behind the magnetic obstacles, the velocity component in the x-direction is shown in Fig. 4 as a function of time at two distinct points located on the central line of each

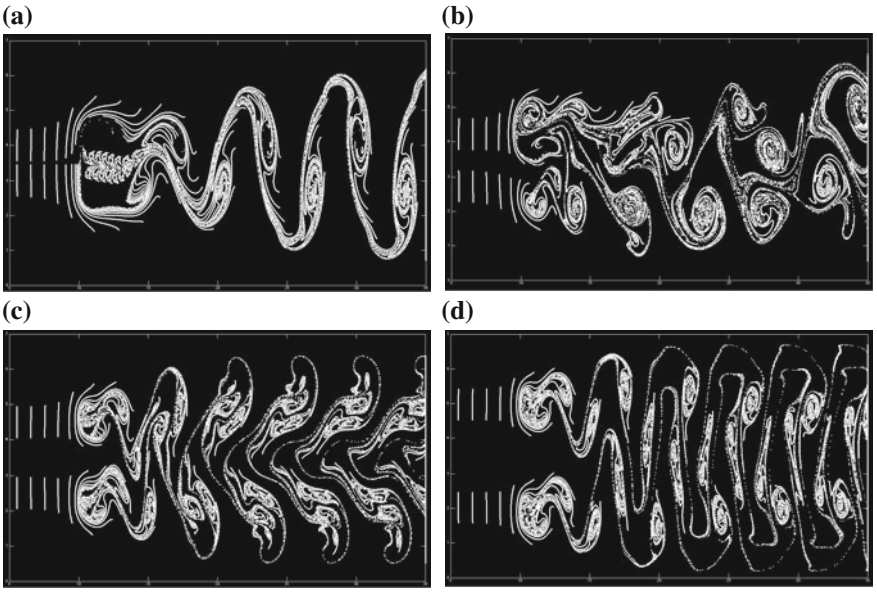

Fig. 3 Lagrangian tracking of the numerically calculated flow past a pair of magnetic obstacles side by side at different separation distances. $Re = 1{,}000$. **a** D = 1, $Q = 2.7$. **b** D = 1.5, $Q = 2.9$. **c** D = 2, $Q = 2.4$. **d** D = 3, $Q = 2.3$

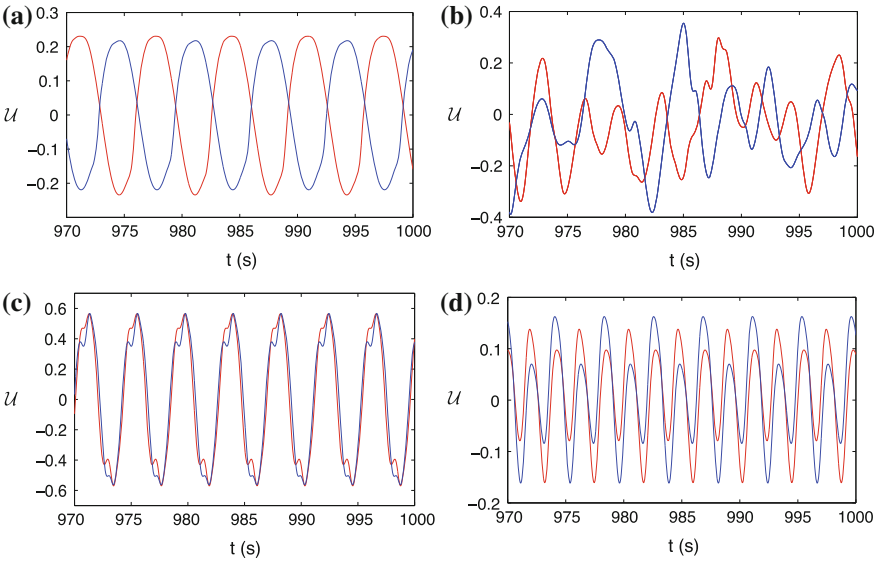

Fig. 4 Velocity component in the x-direction as a function of time at two different points. *Blue* (*red*) line corresponds to the point located at the central line of the *upper* (*lower*) obstacle five dimensionless units downstream. $Re = 1{,}000$. **a** $D = 1$, $Q = 2.7$. **b** $D = 1.5$, $Q = 2.9$. **c** $D = 2$, $Q = 2.4$. **d** $D = 3$, $Q = 2.3$

obstacle, five dimensionless units downstream. For $D = 1$ (Fig. 4a), corresponding to the single wake of a large magnetic obstacle, the velocity signals oscillate in antiphase. This is consistent with the fact that a large oscillating vortex structure is formed behind the obstacle so that in the symmetrically located points where the signals are registered, the velocity in the x-direction takes opposite values. For $D = 1.5$ which corresponds to the bistable flow, velocity oscillations do not present a defined structure. This seems to be a characteristic feature of this regime as it has been reported in the literature for the case of circular cylinders (Zdravkovich 1985; Peschard and Gal 1996). Figure 4c clearly shows in phase oscillations of the velocity signals when $D = 2$ where even the amplitude of the oscillations coincides. Finally, when $D = 3$ (Fig. 4d), although velocity oscillations are in phase, amplitudes do not coincide which indicate a weaker coupling of the wakes.

Important information can also be obtained from the Fourier analysis of the temporal behavior of the velocity signals, particularly for determining the dominant dimensionless frequency of the flow, that is, the Strouhal number. It is precisely at this frequency at which the greatest amount of energy in the flow is transported. Figure 5 shows the power spectrum obtained through the fast Fourier transform of the corresponding velocity signals presented in Fig. 4 for different values of D. Only the spectrum at one point is shown since it coincides with the one at the other point. In Fig. 5a ($D = 1$), a clear dominant characteristic frequency of 0.152 and its corresponding harmonics are shown. This frequency is close to the ones obtained

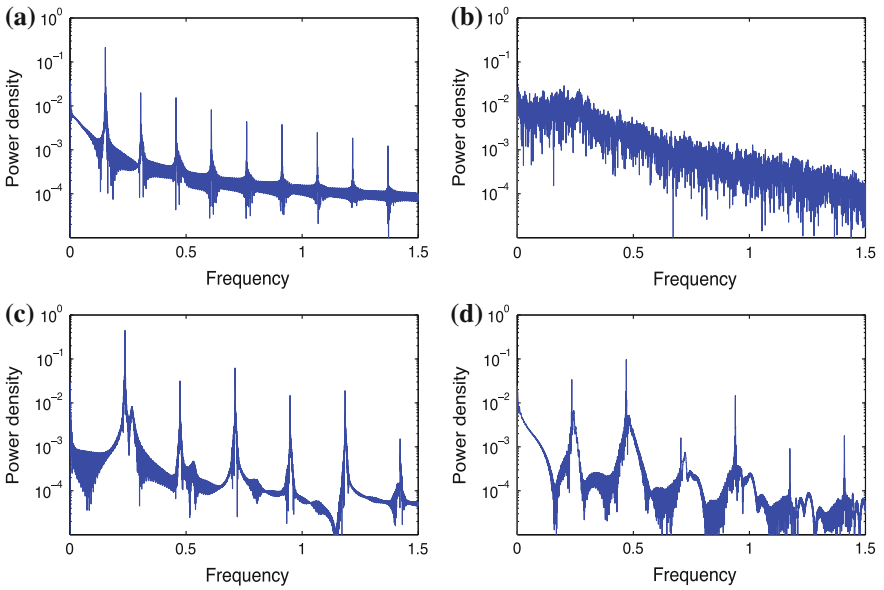

Fig. 5 Power spectrum calculated by the Fast Fourier Transform of the velocity signals presented in Fig. 4. $Re = 1{,}000$. **a** $D = 1$, $Q = 2.7$. **b** $D = 1.5$, $Q = 2.9$. **c** $D = 2$, $Q = 2.4$. **d** $D = 3$, $Q = 2.3$

experimentally by Honji and Haraguchi (1995) for the flow past a single magnetic obstacle. Further, it almost coincides with the value of 0.150 corresponding to the flow past a solid cylinder (Zdravkovich 1997). For the bistable flow at $D = 1.5$ (Fig. 5b), it does not exist a clear dominant frequency since this local analysis does not capture the global behavior of the biased flow that may present two distinct characteristic frequencies for the vortex shedding. Finally, Fig. 5c,d display very similar Strouhal numbers of 0.235 and 0.237 for $D = 2$ and $D = 3$, respectively. It could be expected that for a large enough separation distance, the dominant frequency of each wake should be close to that of a single magnetic obstacle ($\approx$0.152). The difference with the latter case for $D = 2$ and $D = 3$ manifests that the coupling of the wakes is still present at these separation distances. In fact, for the flow past a pair of solid cylinders side by side, the uncoupling of the wakes is observed at $D \approx 5.5$ (Le Gal et al. 1990).

A characteristic feature of the bistable regime is the tendency of the flow in the gap between the obstacles to tilt towards one obstacle at a given time and towards the other obstacle at a later time. This deflection breaks the symmetry of the flow pattern (Le Gal et al. 1990). Figure 6 illustrates this phenomenon through the instantaneous velocity fields at two different times for the bistable regime observed when $D = 1.5$.

Although in previous results only time-dependent flows were considered, at lower values of Q steady flow patterns displaying a vortex pair are found (Román 2013). With the aim of describing the studied flow in a more complete way, Fig. 7 presents a map that shows the regions of steady and time-dependent behavior in terms of the analyzed values of Q and D, for $Re = 1{,}000$. The transition zone between steady and unsteady flows is presented with a gray strip since it is not possible to determine an exact value for this transition. This map is built based on the time behavior of the velocity signals. It is observed that for a fixed D, vortex shedding disappears as Q decreases.

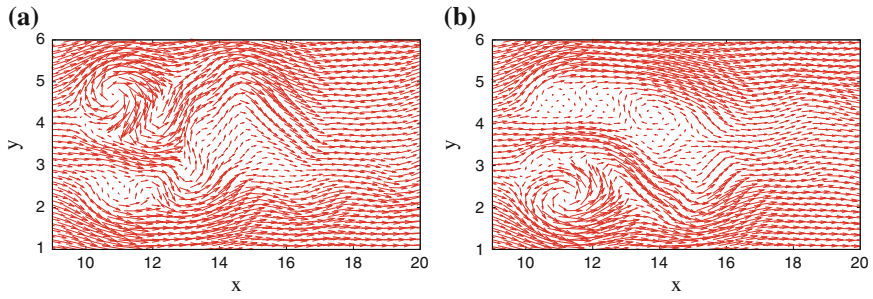

Fig. 6 Instantaneous velocity fields for the bistable regime. $Re = 1{,}000$, $Q = 2.9$ and $D = 1.5$. **a** $t = 1975$, **b** $t = 1992$

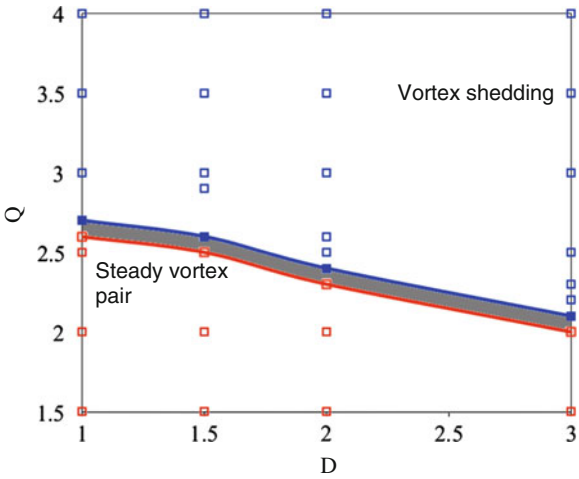

Fig. 7 Stability map of the flow past a pair of magnetic obstacles side by side. The *gray* strip displays the transition zone between steady and time-dependent flow. $Re = 1{,}000$

4 Concluding Remarks

In this work, we have investigated numerically using a Q2D model the flow past a pair of magnetic obstacles side by side at a fixed Reynolds number, $Re = 1{,}000$. We analyzed the coupling of the wakes behind the magnetic obstacles under vortex shedding conditions for different values of the dimensionless separation distance, namely, $D = 1$, 1.5, 2, and 3. From the numerical velocity field, Lagrangian trajectories were obtained which allow to visualize different flow structures. A strong coupling was found for $D = 1$ where the pair of obstacles act as a large magnetic obstacle that produces a single wake whose dominant frequency is close to the one found experimentally (Honji and Haraguchi 1995) and almost coincide with that of the flow past a solid cylinder. A more complex pattern was found for $D = 1.5$ where an intermediate coupling leads to a bistable regime, characterized by a biased flow with asymmetric flow structures. Finally, a weaker coupling of the wakes was found for $D = 2$ and $D = 3$, where well defined in phase wakes are observed. In general terms, it can be stated that the flow past a pair of magnetic obstacles side by side presents similar regimes as those observed in the wakes created by a pair of solid cylinders.

Acknowledgments This work has been supported by CONACyT, Mexico, under project 131399. J. Román also acknowledges a grant from CONACyT. The authors are grateful to Saul Piedra for providing the subroutine for the particle tracking that we present in this article.

References

Afanasyev YD, Korabel VN (2006) J Fluid Mech 553:119–141
Beltrán A (2010) Flow dynamics in magnetic obstacles. PhD thesis, National Autonomous University of Mexico
Cuevas S, Smolentsev S, Abdou MA (2006) J Fluid Mech 553:227–252
Figueroa A, Demiaux F, Cuevas S, Ramos E (2009) J Fluid Mech 641:245–261
Honji H (1991) J Phys Soc Jpn 60(4):1161–1164
Honji H, Haraguchi Y (1995) J Phys Soc Jpn 64(7):2274–2277
Kenjeres S (2012) Phys Fluids 24:115111
Kenjeres S, ten Cate S, Voesenek CJ (2011) Int J Heat Fluid Flow 32:510–528
Le Gal P, Chauve MP, Lima R, Rezende J (1990) Phys Rev A 41:4566–4569
Le Gal P, Peschard I, Chauve MP, Takedaa Y (1996) Phys Fluids 8(8):2097–2106
McCaig M (1977) Permanent magnets in theory and practice. Wiley, New York
Peschard I, Le Gal P (1996) Phys Rev Lett 77:3122–3125
Román J (2013) Numerical study of the heat transfer in flows past arrays of magnetic obstacles. MSc thesis, National Autonomous University of Mexico (In Spanish)
Sumner D, Wong SST, Price SJ, Paidoussis MP (1999) J Fluids Struct 13:309–338
Tympel S, Boeck T, Schumacher J (2013) J Fluid Mech 735:553–586
Votyakov EV, Kolesnikov Yu, Andreev O, Zienicke E, Thess A (2007) Phys Rev 98:144504
Votyakov EV, Zienicke E, Kolesnikov Yu (2008) J Fluid Mech 610:131–156
Zdravkovich MM (1985) J Sound Vib 101:511–521
Zdravkovich MM (1997) Flow around circular cylinders, vol I. Oxford University Press, New York
Zhang X, Huang H (2013) ASME J Heat Transf 135:021702